Dynamics of Wind-Turbine Driven Self-Excited Induction Generator with Online Parameter Calculation

Sohail Khan, Mohsin Shahzad, Peter Palensky
Energy Department
Austrian Institute of Technology
Vienna, Austria
{sohail.khan.fl,mohsin.shahzad.fl,peter.palensky}@ait.ac.at

Khurram Jahangir
Department of Electrical Engineering
COMSATS Institute of Information Technology
Abbottabad, Pakistan
engrkhurram@ciit.net.pk

***Abstract*—This paper presents the dynamics of wind-turbine driven Self Excited Induction Generator (SEIG) with the consideration of dynamic core losses and dynamic mutual inductance. The core losses when considered are often taken as function of air-gap voltage and very few researchers included the variation as function of stator synchronous frequency. Similarly in most of the cases mutual inductance is taken as constant which is a simplified version of true dynamics. In this paper simulation studies are carried out to assess the dynamic performance of SEIG considering both the core losses and mutual inductance as dynamic variables. The performance is assessed in presence of variations in rotor speed, simulated as wind's effect, by a simplified wind turbine model. It is observed that dynamic mutual inductance and dynamic rotor losses are important parameters for accurate voltage and current measurements.**

Keywords—Induction Machine; Modeling; SEIG; Dynamic Mutual Inductance; Dynamic Core Losses; Wind Turbine;

I. INTRODUCTION

Future power system is envisioned as a complex system incorporating distributed generation to harness diverse and spatially dispersed renewable energy resources. In this context wind farms are getting increasingly popular. Due to remote and rugged operational specifications of wind turbines they require robust machinery that is cost effective and require low maintenance. SEIG is good candidate for low power remote area applications that have no grid connectivity and loads are not sensitive to frequency deviations [1]. The primary benefit of SEIG is that it is self-excited and does not need external power from grid for excitation. The benefits of SEIG are low cost, brushless rotor operation, low maintenance requirement and simple construction [1]. These advantages enabled SEIG for wide range of applications in isolated wind turbines and micro-hydro turbines [2, 3].

The self-excitation in SEIG is provided by shunt capacitor connected across the stator terminals. If the rotor of SEIG is connected to rotational inertia like wind turbine rotor shaft then the voltage is induced in the rotor due to initial stator DC voltage. This causes rotating magnetic field which results in three phase voltage induction in the stator three phase windings. The increased stator voltage increases the rotor induced voltage which in turn causes the voltage buildup across the stator terminals until the saturation of magnetic flux linkage occurs [4]. During this process the rotor speed must be greater than the synchronous speed (positive slip), corresponding to the desired output frequency, to sustain the induced generation operation. The challenges associated with SEIG in this regard are related to the regulation of output voltage and frequency. Here the frequency is not only the function of rotor speed but it also varies as function of load even when rotor speed is fixed. Power electronics is normally applied to address these challenges but it is not in the scope of this paper.

The concept of self-excitation is known since 1930 [5]. In the start little work has been done as most of the focus remained on the synchronous generators [6]. However last three decades have seen many publications analyzing the dynamics and control of SEIG. The choice of appropriate capacitance value is dealt in [7]. T. F. Chan has analyzed SEIG driven by regulated and unregulated wind turbines in [8]. Wind turbine driven SEIG is also discussed in [9]. In these papers the iron losses and mutual inductance are dealt as constant variables.

This paper deals with the dynamic simulation of SEIG connected to wind turbine based on the model proposed in [10] which includes dynamic iron losses but constant mutual inductance. However, in this paper both the iron losses and mutual inductance are modeled by dynamic variables to simulate true dynamic performance of SEIG. In conventional model of SEIG iron losses are either neglected for simplicity, represented by constant value [11] or linearly dependent on air-gap voltage [12]. However practically iron losses vary as reaction to both air-gap voltage and stator synchronous frequency. Similarly mutual inductance is represented by a constant value as in [13]. But if a loss minimization strategy based on flux adjustment is desired then the exact mutual flux can be useful [14]. Both of these parameters if computed online helps in designing vector control system and increase the confidence during the stability analysis of the control schemes. The dynamic model of SEIG used in this paper is studied in α-β stationary frame which also make it convenient to handle the complexity and helps in computation of time

varying parameters. This paper is exclusively focused on fixed resistive load at the output and variable rotor speed as function of wind turbine dynamics and dynamic analysis of SEIG model.

The paper is organized as follows: In section II, the mathematical models of wind turbine and SEIG are discussed. Section III discusses the corresponding model in the Simulink® and the calculation of dynamic parameters. In Section IV, the results of simulations are discussed to analyze the performance of the system model. In section V, the summary of paper is concluded and future work is discussed.

II. MATHEMETICAL MODELING

A. Wind Turbine Model

The power contained as kinetic energy in the wind crossing the surface area A with speed V_v is [15]

$$P_w = \rho A V_v^3 / 2 \tag{1}$$

Here ρ is air density taken as 1.225 Kg/m^3. Wind turbine can only extract part of this energy given as

$$P_t = \rho A V_v^3 R^2 \pi C_p / 2 \tag{2}$$

Here R is the radius of wind turbine and C_p is the dimensionless power coefficient expressing the effectiveness of wind turbine in transforming kinetic energy in wind to mechanical energy. The theoretical maximum value of C_p is given by Betz limit [14]

$$C_{p\_theor\_\max} = 0.593 \tag{3}$$

C_p is given as function of tip speed ratio λ and coefficient of torque C_t

$$C_p = \lambda C_t \tag{4}$$

Here λ as function of angular speed of rotor ω_r is

$$\lambda = R\omega_r / V_v \tag{5}$$

The fundamental resonance frequency of the drive train can be sufficiently modeled by a two mass model as given in [14]. But for the sake of simplicity the rotational speed of the rotor is directly used after conversion from the gear ratio. This rotor speed is then fed into SEIG model.

B. SEIG Model

The SEIG model used in this paper is a two axis model also called as α-β model. The transformation is given as [16]

$$\begin{bmatrix} f_\beta^s \\ f_\alpha^s \\ f_0^s \end{bmatrix} = \frac{2}{3} \begin{bmatrix} \cos\theta & \cos(\theta - 2\pi/3) & \cos(\theta + 2\pi/3) \\ \sin\theta & \sin(\theta + 2\pi/3) & \sin(\theta - 2\pi/3) \\ 1/2 & 1/2 & 1/2 \end{bmatrix} \begin{bmatrix} f_a^s \\ f_b^s \\ f_c^s \end{bmatrix} \tag{6}$$

Where θ is the displacement of two-axis model i.e. α-β axis from three-axes model i.e. abc-axes. f_0^s is the same as zero axis component in a three phase system and s represents the stationary frame. The rotating reference frame is related to static frame [17] as

$$\begin{bmatrix} f_\beta^e \\ f_\alpha^e \end{bmatrix} = \begin{bmatrix} \cos\theta & -\sin\theta \\ \sin\theta & \cos\theta \end{bmatrix} \begin{bmatrix} f_\beta^s \\ f_\alpha^s \end{bmatrix} \tag{7}$$

Here θ as function of angular speed $\omega(t)$ and initial value is

$$\theta(t) = \int_o^t \omega(t)\,dt + \theta(0) \tag{8}$$

The SEIG model in stationary reference frame [10] is shown in Fig. 1

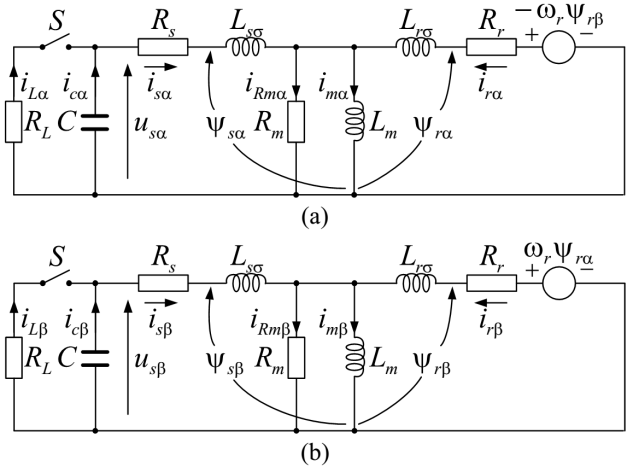

Fig. 1 SEIG model in stationary reference frame: (a) α axis, (b) β axis

The capacitance C connected at the stator side provides the necessary lagging magnetizing current to start the rotor excitation which eventually leads to voltage buildup until the saturation occurs and machine start operating in steady state. The load R_L is connected after some time till the machine stabilized itself. $i_{C\alpha}$, $i_{L\alpha}$, $i_{C\beta}$, $i_{L\beta}$ are the currents in individual capacitor and load branches in both axes. $u_{s\alpha}$ *and* $u_{s\beta}$ represents the voltage across capacitor and have some initial value. The copper losses in stator and rotor are represented by R_s and R_r respectively.

Equations [9-26] are from [10] unless specified otherwise. The leakage flux inductance at stator and rotor sides is represented by $L_{s\sigma}$ *and* $L_{r\sigma}$. $\Psi_{s\alpha}$ and $\Psi_{r\alpha}$ is the stator and rotor flux linkages given as

$$\Psi_{s\alpha} = L_{s\alpha} i_{s\alpha} + L_m i_{m\alpha} \tag{9}$$

$$\Psi_{r\alpha} = L_{r\alpha} i_{r\alpha} + L_m i_{m\alpha} + \Psi_{r\beta o} \tag{10}$$

$\Psi_{r\beta o}$ represents the residual rotor flux. Similarly in β axis

$$\Psi_{r\beta} = L_{r\beta} i_{r\beta} + L_m i_{m\beta} \tag{11}$$

$$\Psi_{r\beta} = L_{r\beta} i_{r\beta} + L_m i_{m\beta} + \Psi_{r\alpha o} \tag{12}$$

$$u_{s\alpha} = R_s i_{s\alpha} + \frac{d\Psi_{s\alpha}}{dt} \tag{13}$$

$$u_{s\beta} = R_s i_{s\beta} + \frac{d\Psi_{s\beta}}{dt} \tag{14}$$

Air gap flux linkage is given as [15]:

$$\Psi_{m\alpha} = L_m i_{m\alpha} = \frac{R_m L_m}{R_m + sL_m}\left(i_{s\alpha} + i_{r\alpha}\right) \tag{15}$$

$$\Psi_{m\beta} = L_m i_{m\beta} = \frac{R_m L_m}{R_m + sL_m}\left(i_{s\beta} + i_{r\beta}\right) \tag{16}$$

The dynamics of the currents are modeled as follows:

$$i_{s\alpha} = -\left(\frac{R_s}{L_{\sigma s}} + \frac{R_m}{L_m} + \frac{R_m}{L_{\sigma s}}\right)\frac{i_{s\alpha}}{s} - \frac{R_s R_m}{L_{\sigma s} L_m}\frac{i_{s\alpha}}{s^2} - \frac{R_m}{L_{\sigma s}}\frac{i_{r\alpha}}{s} - \frac{1}{L_{\sigma s}}\frac{u_{s\alpha}}{s} - \frac{R_m}{L_{\sigma s} L_m}\frac{u_{s\alpha}}{s^2} \tag{17}$$

$$i_{s\beta} = -\left(\frac{R_s}{L_{\sigma s}} + \frac{R_m}{L_m} + \frac{R_m}{L_{\sigma s}}\right)\frac{i_{s\beta}}{s} - \frac{R_s R_m}{L_{\sigma s} L_m}\frac{i_{s\beta}}{s^2} - \frac{R_m}{L_{\sigma s}}\frac{i_{r\beta}}{s} - \frac{1}{L_{\sigma s}}\frac{u_{s\beta}}{s} - \frac{R_m}{L_{\sigma s} L_m}\frac{u_{s\beta}}{s^2} \tag{18}$$

$$i_{r\alpha} = -\frac{R_m i_{s\alpha}}{L_{\sigma r} s} - \left(\frac{R_r}{L_{\sigma s}} + \frac{R_m}{L_m} + \frac{R_m}{L_{\sigma r}}\right)\frac{i_{r\alpha}}{s} - \frac{\omega_r i_{r\beta}}{s} - \frac{\omega_r R_m i_{s\beta}}{L_{\sigma r} s^2} - \frac{R_r R_m i_{r\alpha}}{L_{\sigma r} L_m s^2} - \frac{\omega_r R_m i_{r\beta}}{s^2}\left(\frac{1}{L_{\sigma r}} + \frac{1}{L_m}\right) - \frac{K_{r\alpha}}{L_{\sigma r} s} - \frac{R_m K_{r\alpha}}{L_{\sigma r} L_m s^2} \tag{19}$$

$$i_{r\beta} = -\frac{R_m i_{s\beta}}{L_{\sigma r} s} - \left(\frac{R_r}{L_{\sigma s}} + \frac{R_m}{L_m} + \frac{R_m}{L_{\sigma r}}\right)\frac{i_{r\beta}}{s} + \frac{\omega_r i_{r\alpha}}{s} + \frac{\omega_r R_m i_{s\alpha}}{L_{\sigma r} s^2} - \frac{R_r R_m i_{r\beta}}{L_{\sigma r} L_m s^2} + \frac{\omega_r R_m i_{r\alpha}}{s^2}\left(\frac{1}{L_{\sigma r}} + \frac{1}{L_m}\right) + \frac{K_{r\beta}}{L_{\sigma r} s} + \frac{R_m K_{r\beta}}{L_{\sigma r} L_m s^2} \tag{20}$$

Core loss current can be computed as

$$R_m i_{Rm\alpha} = L_m \frac{di_{m\alpha}}{dt} \tag{21}$$

$$R_m i_{Rm\beta} = L_m \frac{di_{m\beta}}{dt} \tag{22}$$

The magnetization currents can be obtained as follows

$$i_{m\alpha} = i_{s\alpha} + i_{r\alpha} - i_{Rm\alpha} \tag{23}$$

$$i_{m\beta} = i_{s\beta} + i_{r\beta} - i_{Rm\beta} \tag{24}$$

The stator voltages can be obtained as

$$u_{s\alpha} = u_{c\alpha} = \frac{1}{C}\int_0^t i_{c\alpha} dt + u_{s\alpha o} \tag{25}$$

$$u_{s\beta} = u_{c\beta} = \frac{1}{C}\int_0^t i_{c\beta} dt + u_{s\beta o} \tag{26}$$

Here $u_{s\alpha o}$ and $u_{s\beta o}$ are the initial capacitor voltages that also provide starting values for the simulation. $K_{r\alpha}$ and $K_{r\beta}$ represent the residual voltages in the rotor in both the axes.

III. SIMULINK MODEL

The Simulink model of the system consists of two parts i.e. the wind turbine model and SEIG model as shown in Fig. 2

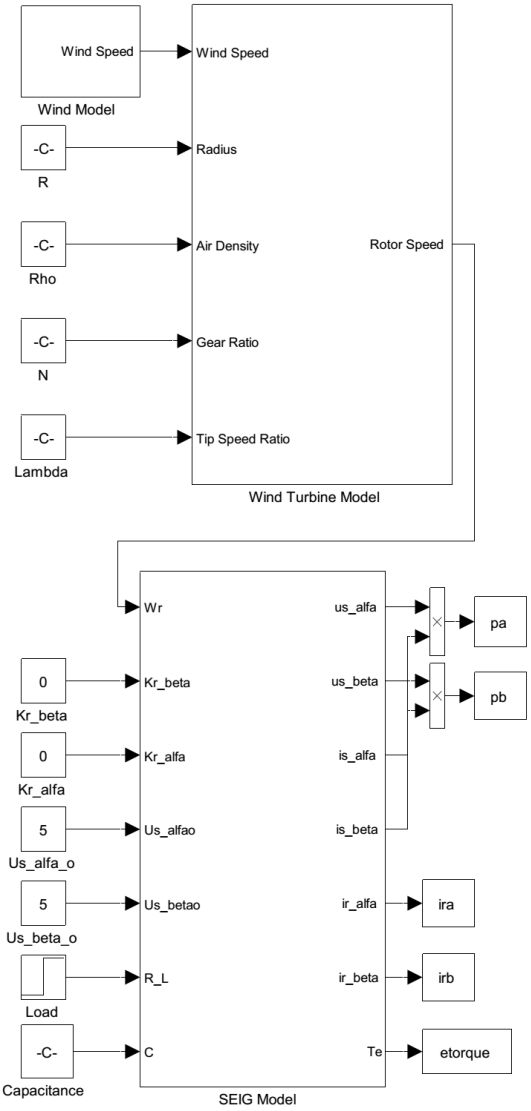

Figure 2: Simulink Model of Overall System

A. Dynamic Core Loss Resistance

The core loss resistance R_m is modeled as function of synchronous frequency at stator and air-gap flux. The air-gap flux is represented by the core loss current and it is computed from equations 21 and 22 using following relationship [15]:

$$i_{Rm} = \frac{\sqrt{i_{Rm\alpha}^2 + i_{Rm\beta}^2}}{\sqrt{2}} \tag{27}$$

The stator synchronous frequency is obtained as follows [10]

$$\omega_s = \frac{d}{dt}\left(\tan^{-1}\left(\frac{u_{s\alpha}}{u_{s\beta}}\right)\right) \tag{28}$$

R_m is computed from a lookup table constructed from test data computed offline using standard no-load tests. It is the function of core loss current i_{Rm} and stator synchronous frequency and shown in Fig. 3.

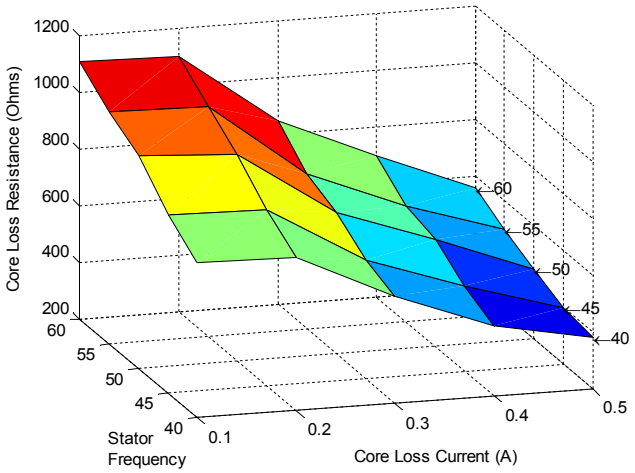

Figure 3: Core Loss Resistance

B. Dynmaic Mutual Inductance

SEIG usually operates in saturation region thus the accurate measurement of mutual inductance is important for dynamical analysis. It is measured for test machine using no load tests [15]. L_m is obtained from the linear interpolation of the test data of mutual inductance plotted as function of magnetizing current I_m. The test data is approximated by two polynomial curves fits.

If $I_m < 1.157A$

$$L_m = (0.06)*(I_m^4) - (0.14)*(I_m^3) + (0.012)*(I_m^2) + (0.125*I_m) + 0.23 \tag{29}$$

If $I_m \geq 1.157A$

$$L_m = (4*10^{-6})*(I_m^4) - (2.4*10^{-4})*(I_m^3) + (5.5*10^{-3})*(I_m^2) - (0.0605*I_m) + 0.3552 \tag{30}$$

In the next section the simulation results are discussed.

IV. Simulation Analysis

The system is simulated for a wind profile shown in Fig. 5. The wind speed directly corresponds to the rotor speed. Starting from a stand still start the speed increasing linearly till time $t=4$ seconds. It encounters a wind gust that increases the speed of rotor momentarily. From $t=10$ seconds onwards the wind is assumed to have a constant value to observe the steady state dynamics of the machine.

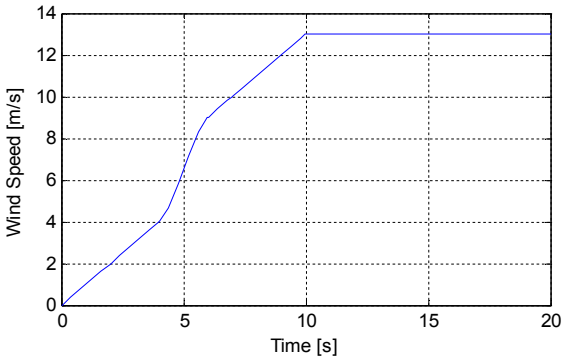

Figure 4: Wind Speed Dynamics for Test Case

Fig. 5 compares the true value of dynamic mutual inductance L_m to the fixed case.

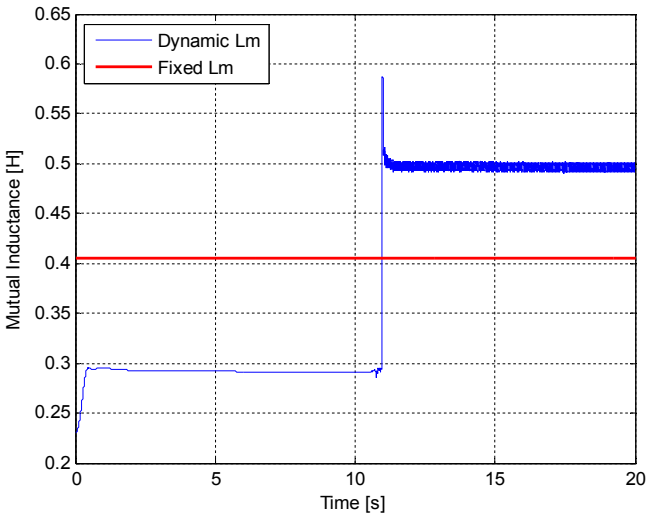

Figure 5: Mutual Inductance (L_m) Dynamics

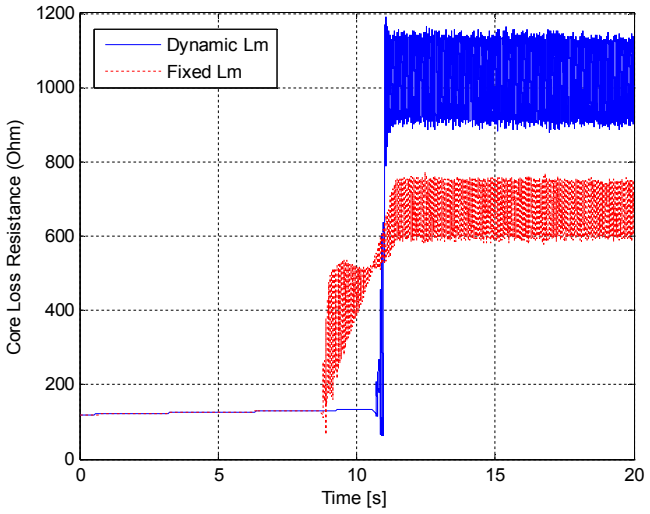

Figure 6: Core Loss Resistance Dynamics

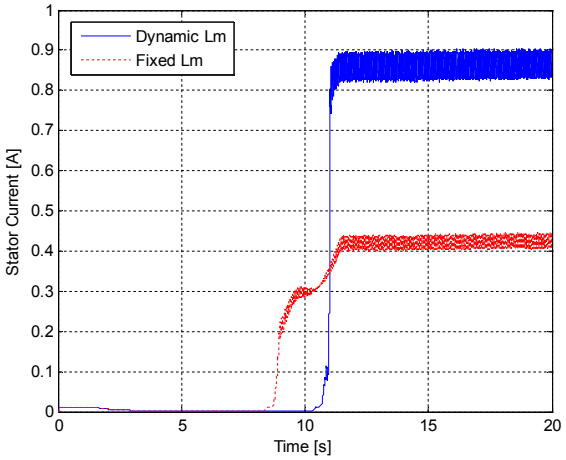

Figure 7: Stator Voltage Dynamics

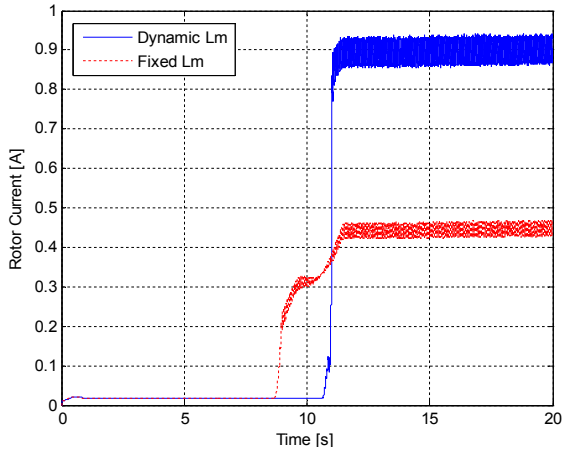

Figure 8: Rotor Current Dynamics

Fig. 6 indicates the effect of dynamic mutual inductance L_m on dynamic core loss resistance R_m. It shows an error of *32.6*% in computation of R_m for (t > *12* sec) for *18.2*% difference between L_m. In Fig. 7 and 8, there is significant difference between steady state current values which is due to difference between mutual inductance values for both cases in reference to Fig. 5. The stator voltage dynamics and rotor current dynamics are almost similar because of the assumption of fixed and resistive load.

V. CONCLUSION

In this paper simulation studies are carried out to assess the significance of considering the mutual inductance as a dynamic parameter. Meanwhile dynamics of core loss resistance also influences the simulation results. It is observed that there is a considerable error in computation of observed variables like stator and rotor currents that is proportional to error in mutual inductance. As in the steady state, an error of *49%* is observed in rotor induced current corresponding to *18%* difference between L_m for *(t > 12 sec)*. If L_m is chosen corresponding to steady state rotor speed in the saturation region then the complexity of model can be reduced. But significant information can be lost during transients in the rotor speed which can be important for stability analysis. For future work, it is suggested to consider noise and thermal effects in parameter calculations to enhance the existing model. The wind turbine model can be enhanced to include the effect of resonance on machine dynamics. Moreover the system can be analyzed with inductive loads to observe its effects on machine dynamics.

APPENDIX

$L_{\sigma s}$= 0.01823 H, $L_{\sigma r}$= 0.01823 H, R_s = 4.293 Ω, R_r = 3.866 Ω, L_m = 0.4058 H, C = 50μF, R_L = 100 Ω [10]

REFERENCES

[1] Seyoum, D.; Grantham, C.; Rahman, M.F., "The dynamic characteristics of an isolated self-excited induction generator driven by a wind turbine," Industry Applications, IEEE Transactions on , vol.39, no.4, pp.936,944, July-Aug. 2003.

[2] Murthy, S.S.; Malik, O. P.; Tandon, A.K., "Analysis of self-excited induction generators," Generation, Transmission and Distribution, IEE Proceedings C , vol.129, no.6, pp.260,265, November 1982.

[3] Faria, J.; Margato, E.; Resende, M.J., "Self-Excited Induction Generator for Micro-Hydro Plants Using Water Current Turbines Type," Telecommunications Conference, 2005. INTELEC '05. Twenty-Seventh International , vol., no., pp.107,112, Sept. 2005.

[4] Ojo, O., "The transient and qualitative performance of a self-excited single-phase induction generator," Energy Conversion, IEEE Transactions on , vol.10, no.3, pp.493,501, Sep 1995.

[5] Wagner, C. F., "Self-excitation of induction motors," Electrical Engineering , vol.58, no.2, pp.47,51, Feb. 1939.

[6] Lai, Loi Lei, and Tze Fun Chan. Distributed generation: Induction and permanent magnet generators. Wiley, 2008.

[7] Malik, N.H.; Al-Bahrani, A. H., "Influence of the terminal capacitor on the performance characteristics of a self excited induction generator," Generation, Transmission and Distribution, IEE Proceedings C , vol.137, no.2, pp.168,173, Mar 1990.

[8] Chan, T.F., "Self-excited induction generators driven by regulated and unregulated turbines," Energy Conversion, IEEE Transactions on , vol.11, no.2, pp.338,343, Jun 1996.

[9] Raina, G.; Malik, O. P., "Wind Energy Conversion Using a Self-Excited Induction Generator," Power Engineering Review, IEEE , vol.PER-3, no.12, pp.47,48, Dec. 1983.

[10] Bašić, Mateo, Dinko Vukadinović, and Duško Lukač. "Novel dynamic model of self-excited induction generator with iron losses." International Journal of Mathematical Models and Methods in Applied Sciences 5, 221-229, 2011.

[11] Leidhold, R.; Garcia, G.; Valla, M.I., "Field-oriented controlled induction generator with loss minimization," Industrial Electronics, IEEE Transactions on , vol.49, no.1, pp.147,156, Feb 2002.

[12] Sung-Don Wee; Myoung-Ho Shin; Dong-Seok Hyun, "Stator-flux-oriented control of induction motor considering iron loss," Industrial Electronics, IEEE Transactions on , vol.48, no.3, pp.602,608, Jun 2001.

[13] Idjdarene, K., et al. "Vector control of autonomous induction generator taking saturation effect into account." Energy Conversion and Management 49.10, 2609-2617, 2008.

[14] Abad, G. Doubly Fed Induction Machine: Modeling and Control for Wind Energy Generation. Hoboken, N.J: Wiley, 2011.

[15] Seyoum, Dawit, "The dynamic analysis and control of a self-excited induction generator Driven by a wind turbine," Ph.D. dissertation, Dept. Electrical Eng. & Telecom., UNSW, Sydney, Australia, 2003.

[16] Ong, Chee-Mun. Dynamic simulation of electric machinery: using Matlab/Simulink. Vol. 5. Upper Saddle River, NJ: Prentice Hall PTR, 1998.

[17] Zhong, Qing-Chang, and Tomas Hornik. Control of power inverters in renewable energy and smart grid integration. John Wiley & Sons, 2012.